ACS APPLIED BIO MATERIALS

www.acsabm.org Article

Electrochemical Biosensor Based on L-Arginine and rGO-AuNSs Deposited on the Electrode Combined with DNA Probes for Ultrasensitive Detection of the Gastric Cancer-Related *PIK3CA* Gene of ctDNA

Mahbubur Rahman, Jiaqi Niu, Xinyuan Cui, Cheng Zhou, Ning Tang, Han Jin, and Daxiang Cui*

Cite This: https://doi.org/10.1021/acsabm.2c00393 Read Online

ACCESS | Metrics & More | Article Recommendations | Supporting Information

ABSTRACT: Gene biomarkers of circulating tumor DNA (ctDNA) in liquid biopsies have been explored for use in the precise diagnosis of tumors. There is a great clinical need to realize the ultrasensitive detection of gene biomarkers in ctDNA. Here we reported that an ultrasensitive label-free biosensor was developed for the detection of the gastric cancer-related *PIK3CA* gene of ctDNA in peripheral blood. The polymeric L-arginine and graphene oxide-wrapped gold nanostars (rGO-AuNSs) were prepared and deposited on the glass electrode. The capturing DNA probes for the *PIK3CA* gene were prepared and successfully immobilized on the rGO-AuNS-modified electrode surface via $\pi-\pi$ interaction among the rGO-AuNS composites and DNA probes. The resultant electrochemical sensor was effectively applied to detect the *PIK3CA* gene of ctDNA via the hybridization between the capturing DNA probe and ctDNA, the result of which showed that the biosensor exhibited desirable sensitivity, stability, and a wider dynamic response in a ctDNA concentration range from 1.0×10^{-20} to 1.0×10^{-10} M (R^2 = 0.997). Moreover, the low limit of detection of 1.0×10^{-20} M (S/N = 3) indicates the biosensor owns satisfactory detection sensitivity. Fourteen *PIK3CA* genes and two *PIK3CA* gene mutations were detected in 60 clinical ctDNA samples of gastric cancer patients by using the developed biosensor. In conclusion, this ultrasensitive label-free electrochemical biosensor possesses a significant application prospect in the detection of the *PIK3CA* gene in ctDNA and in early screening for gastric cancer in the near future.

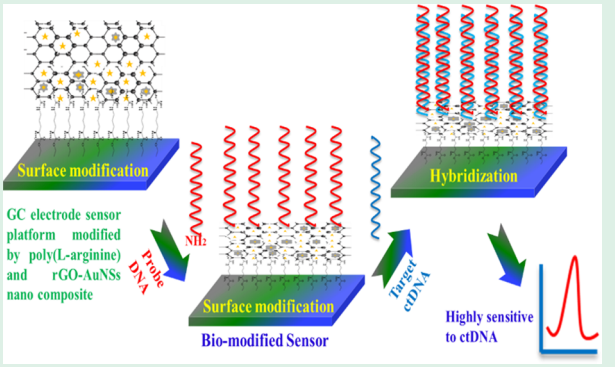

KEYWORDS: *electrochemical biosensor, PIK3CA gene, gastric cancer, circulating tumor DNA (ctDNA), reduced graphene oxide (rGO), gold nanostar (Au NS), liquid biopsy*

INTRODUCTION

Gastric cancer (GC) ranks fifth in cancer incidence and third in cancer mortality worldwide.[1] It is greatly needed in the clinical field to be able to identify gastric cancer patients early. The *PIK3CA* gene is identified as a promising biomarker associated with GC and is confirmed to be third most available mutated gene in gastric cancer.[2] When the *PIK3CA* gene is detected as being overexpressed in gastric cancer, sorafenib is recommended as a target therapeutic drug. When the *PIK3CA* gene is detected to have a gene mutation, 5-Aza is recommended as the target therapeutic drug.

To discover early gastric cancer, liquid biopsy has become a hotspot. For example, the detection of circulating tumor DNA (ctDNA) in the peripheral blood can be used to diagnose tumors and direct tumor therapy.[3−5] The availability and levels of circulating tumor DNA are important indicative factors of the tumor growth and malignant progression.[6] The double helix ctDNA fragments in the cell-free fraction of the blood carry tumor-specific gene mutations that can be used to identify specific cancer types.[6,7] In addition, the presence of ctDNA in the cell-free fraction of blood allows for the utilization of small volumes of blood to diagnose tumors instead of a traditional tissue biopsy, providing a minimally invasive and convenient cancer diagnosis protocol. These unique characteristics have made detection of ctDNA an important tool for liquid biopsy, which can substitute other biomarkers to realize specific cancer diagnostics purposes.[6]

The frequently reported detection approaches of ctDNA in blood are generally based on polymerase chain reaction

Received: April 25, 2022
Accepted: August 14, 2022

Scheme 1. Graphical Description of the Biosensor Fabrication for the Electrochemical Detection of *PIK3CA* Gene of ctDNA

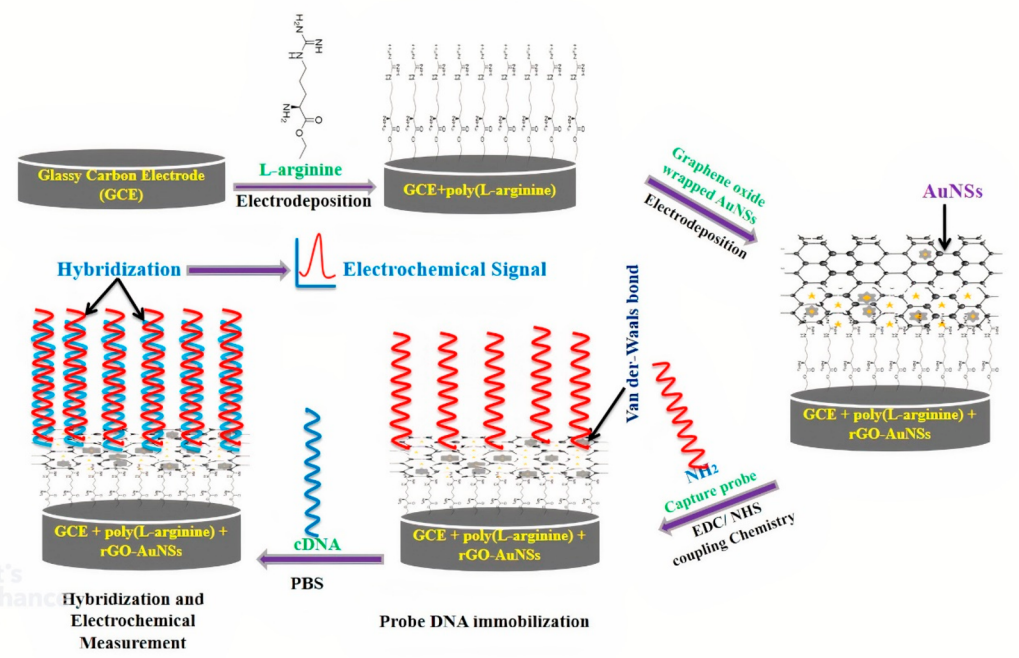

(PCR). Those ctDNA analysis techniques have to face challenges such as specificity, sensitivity, and a low limit of detection (LOD).[4] Although these methods have made remarkable contributions for amplifying ctDNA, the complex sampling and analyzing procedures still need to be improved, particularly with regard to the interference with other components presented in tumor microenvironments.[8] Other usually reported ELISA and HPLC-based techniques for biomarker detection need sophisticated instrumentation, slow detection efficiency, and expensive reagents in each trial.[8]

To date, biosensors shows significant advantages in the detection of cancer biomarkers, and have the potential to improve and avoid the aforementioned limitations.[9] Nowadays, gene-based biosensors attract more and more attention thanks to diverse applications in various aspects of early cancer detection, tumor burden and malignant progression identification, forensic report investigation, and environmental parameter monitoring.[10,11] One particularly promising method involves the use of electrochemical technique for specific gene sequence detection at very low physiological levels, being presented as convenient and effective tools among other gene-based methods.[12] This holds true when compared with other previously reported chemiluminescence and optical biosensor-based methods, as the later have some shortcomings that increase the cost and complexity in sampling and detection.[3] Because of these merits, label-free and enzyme-free electrochemical methods have attracted increasing attention and have been used broadly in gene detection, resulting in an optimization of costs and detection times.[11] With the continuous improvement of surface chemistry and versatile application in the biosensor detection field, nowadays poly(L-arginine)-modified electrodes have achieved remarkable attention in the fabrication of biosensors. L-Arginine monomers (L-arg) can be easily fitted on the surface of a glass carbon electrode by polymerization reaction through the aggregation of their amine and carboxylic functional groups.[13−15] The resulting polymer films on the electrode surface can significantly increase the specificity of the biosensor performance as well as enhance the electron transfer characteristics of the analyte.

With the increasing demand for improved LOD and sensitive detection techniques, sandwich-type assays have been used extensively for increasing the active surface area, permitting a larger amount of probe immobilization on the surface that in turn enhances the detection sensitivity of the fabricated biosensors.[4] Graphene oxide (rGO) together with polymer composite structures has been demonstrated to be very effective for enhancing the electrocatalytic behavior of the modified electrodes.[14,16] The combination of a polymer composite of modified graphene alongside redox couples significantly enhances the catalytic activity due to a rapid electron transfer rate based on their structural roughness.[4] Thus, polymeric bedded graphene-based sensors have better advantage in electrochemical measurements comparing with other functional materials-based sensors.[17] Two-dimensional (2D) graphene oxide-based materials with tunable oxygen functionalities provide an excellent sensing platform to perform high sensitive and specific detection of biomarkers.[13] Graphene-based materials and anisotropic noble metal nanoparticles offer excellent synergistic properties by increasing the catalytic activity due to rapid electron transfer and increased the active surface area to bind target molecules. Graphene is effectively used in the field of biomedical application as an excellent gene or drug delivery vehicle though its distinctive properties of high electrical conductivity, effective active surface area, mechanical strength, thermal conductivity, $\pi-\pi$ stacking, covalent interaction, Van der Waals force of attraction, biocompatibility, and biological or chemical characteristics.[18]

Highly branched gold nanoparticles (AuNPs) display specific characteristics compared with other anisotropic nanoparticles and can provide optical tunability by changing their geometry. Au nanostars (AuNSs) also offer an effective platform for stem cell tracking, in vivo or vitro diagnostics,

https://doi.org/10.1021/acsabm.2c00393
ACS Appl. Bio Mater. XXXX, XXX, XXX−XXX

photothermal or photodynamic treatment of tumors, bioimaging, and immunotherapy. The assay containing AuNSs and rGO are the most common for the analyzed and applicable materials in electrochemical detection. The incorporation of AuNSs into graphene oxide on the poly(L-arg) bedded surface effectively prevents the agglomeration and restacking of the rGO nanosurface by a process of reduction and helps to achieve the target specificity and sensitivity of the biosensor.[4] In our previous works, we developed a gold nanoparticle-decorated graphene oxide platform for gastric cancer cell detection,[19] electrochemical detection of circulating tumor DNA,[20] salivary SERS sensing,[21] and breath analysis to distinguish early and advanced gastric cancer patients from healthy persons.[22]

In this study, we developed a supersensitive sensor for the gastric cancer-related *PIK3CA* gene detection in the ctDNA in peripheral blood (Scheme 1). To improve the electron transfer ability and high-performance electrochemical response, we prepared and applied a nanocomposite consisting of reduced graphene oxide wrapped around gold nanostar (AuNS-rGO) structures. The proposed sensor combines the advantages of the polymeric film formation of an L-arginine monomer and a AuNS-rGO-modified GC electrode (GCE/P-arg/rGO-AuNS), and the DNA probes capturing the *PIK3CA* gene were immobilized directly on the electrode by Van der Waals interaction. The immobilization of the DNA probes was done with a very simple and fast method using a well-known carbodiimide reaction,[19] which formed a covalent bond and enhanced the immobilization performance on the P-arg/rGO-AuNS-modified GCE surface. The resultant electrochemical sensor was applied to detect the *PIK3CA* gene of ctDNA in the peripheral blood, exhibited high sensitivity and specificity, and has great potential for application in the detection of gene biomarkers of ctDNA for tumor diagnosis.

EXPERIMENTAL SECTION

Chemicals and Reagents. Trisodium citrate, gold (III) chloride ($HAuCl_4$), $AgNO_3$, 1-ethyl-3-(3-dimethylaminopropyl) carbodiimide (EDC), and L-arginine monomer were purchased from Sigma-Aldrich (Japan). N-Hydroxysuccinimide (NHS) was obtained from Sigma-Aldrich (Germany). Ascorbic acid and GO nanosheet were provided by LingFeng Chemical, Shanghai, China. Sodium and potassium phosphate buffer, ethanol, and nitrocellulose filter membrane (0.22 μm) were obtained from Macklin Biochemical, China. For rinsing and preparation, all solutions that used DI water (18.2 MΩ) had an analytical grade. The *PIK3CA* gene-related DNA oligonucleotides of gastric carcinoma were provided by Sangon Bioengineering, Shanghai, China, and are listed below:

ssDNA probe: 5′-AGT GAT TTT AGA GAG-3′;
noncomplementary (ncDNA): 5′-TAC TCC GCG CTA ACG-3′.
one-base mismatched DNA: 5′-CTC TCT AGA ATC ACT-3′;
two-base mismatched DNA: 5′-CTC TCT AGA ATG ACT-3′;
complementary DNA (cDNA): 5′-CTC TCT AAA ATC ACT-3′;

The *PIK3CA* gene-related synthetic oligonucleotide probe (E542 K) of gastric carcinoma was used as the target analyte to detect the specific cDNA.

Apparatus. The well-defined DPV, CV, and EIS measurement techniques were performed using an electrochemical workstation (CHI 760E) including a conventional three-electrode configuration (CH Instrument, Shanghai, China) consisting of a Ag/AgCl reference electrode, a piece of platinum (Pt) wire as a counter electrode and GC working electrode (Ø = 3 mm) respectively. An Ag/AgCl electrode was referred to all the potentials measured in this study. The morphological characterization of all the samples were carried out by using high-resolution field emission SEM (Sirion 200, USA), TEM (Tecnai G2 spirit Biotwin, USA), a multifunctional XPS (AXIS Ultra DLD, Japan), and a multifunctional XRD (3KWD8, Germany).

Synthesis of Colloidal Gold Nanostars (AuNSs). The gold-nanostar nanoparticles were synthesized according to our previously reported method.[23] Briefly, a two-step procedure was used to synthesize the gold-nanostar nanoparticles. First, the seed solution of the gold-nanostars (AuNSs) was prepared using a modified seed-mediated growth method.[20] Gold seeds (12 nm) were prepared by boiling a 100 mL solution of 1 mM $HAuCl_4$, then 15 mL of trisodium citrate (1%) was mixed into the solution and stirred vigorously. The solution was then cooled to ambient temperature after being kept boiling for another 15 min. The resultant seed was then filtered using a nitrocellulose membrane (0.22 μm) and stored in the refrigerator for future usage. Second, for the synthesis of colloidal AuNSs, 10 mL of 0.25 mM $HAuCl_4$ solution was mixed with the as-prepared 100 μL gold seed solution. Subsequently, 50 μL of 0.1 M ascorbic acid and 100 μL of 2 mM $AgNO_3$ solution were mixed in to the gold solution. To increase the dispersity of the resulting gold nanostars, we mixed a volume of hexadecyltrimethylammonium bromide (100 μL, 0.1 M). The solution of resultant AuNSs was centrifuged at 4000 rpm for 5 min and redispersed in 1−2 mL water for future usage.

Synthesis of the Gold Nanostar-Graphene Oxide (AuNS-rGO) Nanocomposite. The AuNS-rGO nanocomposites were synthesized according to our previous reports.[20−22] Briefly, to synthesize the AuNS-rGO nanocomposite, a 0.3 mg/mL graphene oxide nanosheet was dispersed in 0.1 M PBS buffer at pH 7.4 and stirred for 20 min; the dispersion was then sonicated for 1 h. Later, a 3 mg/mL AuNS solution was added in the GO solution and sonicated for another 15 min. The resulting GO nanosheet wrapped AuNS nanocomposite was stored for future usage.

Fabrication of the Working Electrode. A GC (diameter of 3 mm) working electrode was modified sequentially by a layer-by-layer film fabrication through depositing as-prepared nanosamples as shown in Scheme 1. The surface of the GC electrode was polished properly by alumina slurries with water (size 0.3 μm down to 0.05 μm), and then sonicated two times with DI water. The electrode was then sonicated again with ethanol and finally properly rinsed with DI water and allowed to dry under nitrogen gas.

After cleaning, the surface was electrochemically activated by running cyclic voltammetry (ranging from −0.2 V to +1.6 V with a 0.1 V s^{-1} scan rate) until reproducible voltammograms were obtained vs the reference electrode (Ag/AgCl) in 0.5 M H_2SO_4.[24] The roughness factor of the working electrodes was calculated to be 1.85 ± 0.1 by considering the ratio of the geometric to the real surface area and was kept constant throughout the study. This value was derived from the peak area associated to the pick current of reduction obtaining from the CV cycle in H_2SO_4 and the monolayer of the chemically absorbed oxygen. Characterization of the activated GC electrode surface was done by cyclic voltammetry methods with the applied voltage between −0.2 V to +1.6 V vs a reference electrode (Ag/AgCl) with a 0.1 V s^{-1} scan rate. EIS was measured in Ferri-ferrocyanide (2 mM) in 0.1 M KCl electrolytic solution. The electrochemical characterization was performed by well-defined EIS and CV methods after each and every step of the surface modification procedure.

L-arginine monomer was diluted in PBS buffer solution (0.1 M and pH 7.4) and electropolymerized on the electrochemically cleaned GC electrode surface by using CV for definite cycles by applying a voltage (range −2.0 V to +2.0 V) at a 100 mV s^{-1} scan rate. After poly(L-arginine) film formation, the electrode (GCE/P-arg) was rinsed carefully with water and then dried in the open air. The rGO-AuNS nanocomposite was then electrochemically deposited on the modified electrode (GCE/P-arg) and kept in a deoxygenated conditions by observing releasing of N_2 bubbling. Fourteen CV cycles were run by applying a voltage between −2.0 V and +2.0 V vs a reference electrode (Ag/AgCl) at a 0.05 V s^{-1} scan rate. Then, electrochemically reduced rGO and concurrently deposited rGO-AuNS nanocomposite GCE were gently rinsed with DI water and allowed to dry in the air. Finally, the modified GCE was kept in the refrigerator at 4 °C, ready for further use. Different modified electrodes were also

https://doi.org/10.1021/acsabm.2c00393
ACS Appl. Bio Mater. XXXX, XXX, XXX−XXX

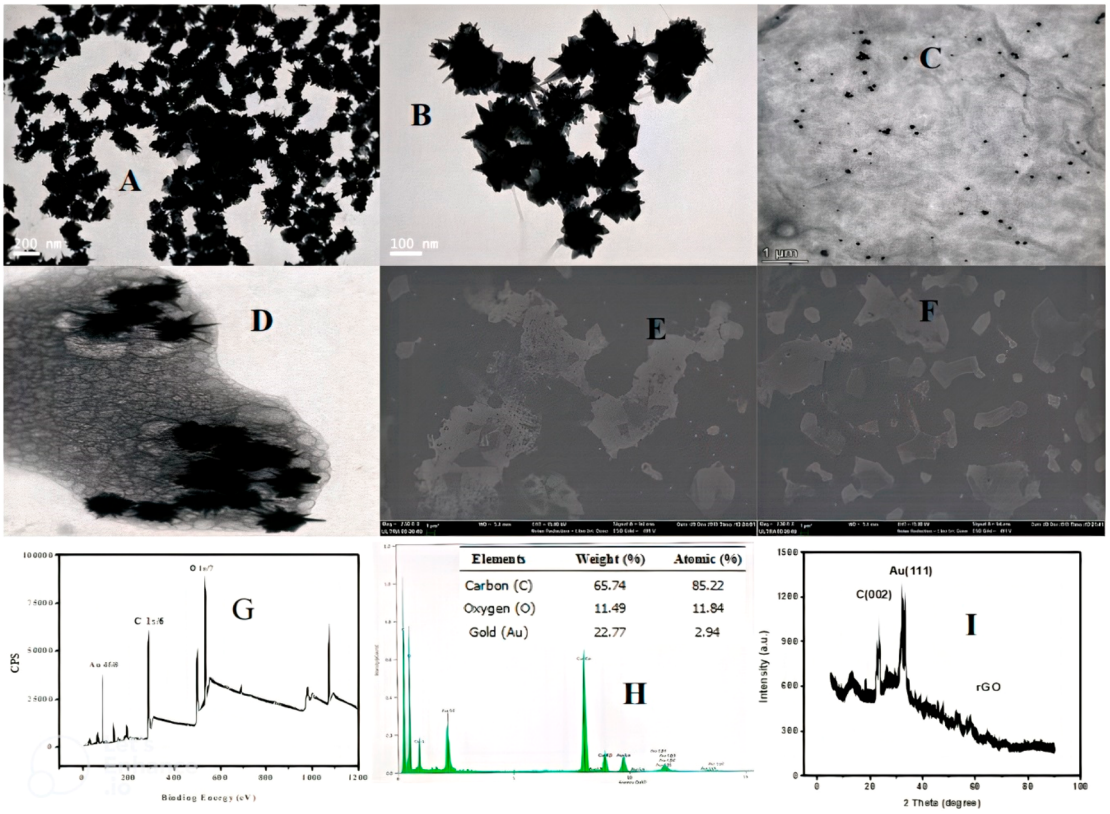

Figure 1. (A) Low- and (B) high-resolution TEM images of AuNSs; (C) low- and (D) high-resolution TEM images of ErGO-AuNS nanocomposite; (E, F) high-resolution SEM images of the GCE/P-arg film; (G) XPS spectrum; (H) TEM EDS spectrum and their corresponding element mapping; and (I) XRD images of rGO-AuNS film.

prepared for surface characterization and the electrochemical performance comparison of the fabricated biosensor.

Optimization of the Experimental Conditions. The catalytic performance of the L-arg+ErGO-AuNS nanocomposite film was significantly reliant on the L-arginine concentration. The concentration of L-arginine was optimized by EIS. By this technique, we could observe that with the increased amount of L-arginine, the electrochemical response of the L-arg+ErGO-AuNS film decreased gradually, with a maximum value at 1 mM L-arginine. With the increased amount of L-arginine on the GC surface, the effective charge transfer was blocked by the thicker film of arginine and decreased the electrochemical response. The redox signal was significantly decreased when the concentration of the L-arginine film was larger than 1.0 mM, which may be associated with much thicker L-arginine film affecting the conductivity of the surface. Therefore, a 1 mM L-arginine concentration was selected for the GCE surface modification of our experiment (see S1 in the Supporting Information). The lower amount of L-arg (lower than 1 mM) resulted in a progressively thinner film on the GCE surface. This may cause a decrease in the number of binding sites of the resulting thin L-arg film with ErGO-AuNSs, leading to the weak physical adsorption between L-arg and rGO-AuNSs.

The electrochemical performance of the GCE/L-arg+ErGO-AuNS-modified electrode was greatly affected by the conditions of preparation and the number of polymerization cycles. Redox signals of the L-arg film modified surface obtained a maximum after 12 electropolymerization cycles, and then gradually decreased with lower or higher number of scans (see S2 in the Supporting Information). Therefore, 12 electropolymerization CV cycles were selected for the GCE surface modification. The potential window was also optimized from −2.0 to 2.0, which demonstrated the most favorable electrochemical preparation conditions for P-arg film formation on the GCE electrode surface comparison with other potential window from −0.6 to 1.6 (see S3 in the Supporting Information). The electrodeposition of ErGO-AuNS nanohybrids was carried out following a previously reported method[13] with some modification. A 0.3 mg/mL concentration of the GO nanosheet was used, and the applied voltage ranged from −1.2 to 0.7 V, which was optimized for rGO-AuNS nanohybrid deposition on the modified GC electrode.

The polished GC electrode modification technique with L-arg and rGO-AuNS composites was optimized. The drop-coated L-arg and GO-AuNS composite was unstable and showed less conductivity, hindering the electron transfer because of a lack of covalent bonding with the electrode surface. The electropolymerized L-arg and electrochemically deposited GO-AuNS composite on the GCE were more stable through the direct linking by C−N covalent bond formation. This resulted in higher conductivity and stability to facilitate the electron transfer pathway (see S4 in the Supporting Information).

DNA Immobilization and Hybridization. Twenty microliters of probe ssDNA (1 μM) was added in PBS buffer solution for dilution at pH 7.4 and then pipetted out on the GCE/P-arg/ErGO-AuNS nanoplatform. The resulting mix was air-dried. After immobilization, the GCE/P-arg/ErGO-AuNS/ssDNA electrode was carefully rinsed with DI water to wash out the DNA probe that was not immobilized. Then, 10 μL of cDNA diluted in PBS buffer at physiological pH was added dropwise onto the top of the GCE/P-arg/ErGO-AuNS/ssDNA electrode and kept in open air drying. After it was dried, the CV was run for 300 s at a fixed voltage of −0.7 V for the hybridization event of ctDNA with the probe DNA, which induces the resulting dsDNA release from the modified GCE surface. Before this electrochemical measurement, the electrode was rinsed properly to remove the unbound oligos. A similar immobilization and hybridization procedure were performed for the selectivity study by testing with a noncomplementary and mismatched DNA sequence. EIS, CV, and

https://doi.org/10.1021/acsabm.2c00393
ACS Appl. Bio Mater. XXXX, XXX, XXX−XXX

DPV measurements were performed after each and every modification step.

Electrochemical Detection Protocol. The electrochemical detection of the *PIK3CA* gene in ctDNA samples was done according to our previous reports.[19−22] Briefly, 2 mM ferri-ferrocyanide in 0.1 M KCl was used for performing the EIS measurements. The EIS AC voltage amplitude was set at 5 mV with a 10 000 to 0.1 Hz frequency range. For the CV measurement, the same electrolyte solution was also applied and the voltage was set from −0.6 V to +0.2 with 0.1 V/s as the scan rate. Oxygen was removed from the system by running a continuous N_2 gas flow for the entire duration of all measurements. Three replicates were measured for every electrode, reporting the mean of three separate analysis. All electrochemical measurements were tested at ambient conditions.

Clinical Sample Examination. Sixty samples of clinical ctDNA from gastric cancer patients were collected from Tangdu Hospital and Shanghai Tongji Hospital, and the *PIK3CA* gene and gene mutation were detected using the developed electrochemical biosensor based on L-arginine and rGO-AuNS deposited on the electrode. This clinical trial was permitted by the hospital ethics committee. Informed consents were signed from the patients with gastric cancer.

RESULTS AND DISCUSSION

Morphological Characterization. Branched gold nanostars (AuNSs) showed a significant optical signal enhancement and demonstrated a surfactant-free pathway for synthesizing emerging biocompatible nanoparticles due to its highly intense nanoantenna effects from the branched sharp features.[22] The term "gold nanostars" usually refers to those nanoparticles with a spherically shaped core from which multiple sharp branches protrude.[4] These shapes show significant properties for their application in two-photon luminescence, plasmonic applications, and surface-enhanced Raman effects. Figure 1A, B shows the overall size of AuNSs is ∼83 nm on average and the sizes of their sharp spikes are ∼4−12 nm.

Figure 1E, F displays the SEM images of the electropolymerized P-arg morphology with a smooth surface. The resulted P-arg film linked directly by forming well-defined covalent bonds (C−N) through carboxylic groups with GC electrode. The rGO-wrapped gold nanostar nanocomposite films (Figure 1C, D) stacked on the GCE/P-arg surface by overlapping with each other.[9] If GO-AuNSs were interconnected with the polymerized P-arg, the obtained P-arg/GO-AuNS composite (Figure 1F) would be formed of stacked nanosheets. The nanosheets were composed of coarse surfaces that evidenced the formation of L-arg agglomerates in the base of GO-AuNS. This resulted in the formation of a rough surface. These observations also confirmed the successful integration of L-arg and GO-AuNS composites by electropolymerization. The XPS spectrum (Figure 1G), TEM EDS spectrum, and their corresponding element mapping show the uniform distribution of AuNSs on the rGO-AuNS composite film (Figure 1H), and the XRD images (Figure 1I) of the rGO-AuNS nanocomposite had the presence of carbon, gold, and oxygen elements in the composite materials.

L-arg and rGO-AuNS Nanocomposite Layer-by-Layer Deposition on GCE Surface. The electropolymerization of L-arg was performed using a CV method with voltage values ranging from −2.0 to +2.0 V and a scan rate set up at 0.1 V s^{-1} for 12 cycles in 0.1 M PBS buffer (pH 7.4) containing 1 mM L-arg solution. A continuous voltammogram of the electrodeposition of L-arg was found on GC electrode (Figure S6A). The increasing redox current with definite CV cycles confirmed the conductive polymeric film formation of L-arg on the bare GCE surface.[23] The α-amino acid free radical was formed by oxidizing the L-arg monomer at a high positive potential, which enhanced the polymerization process. Figure S6A shows that the resulted P-arg film contained more $-NH_2$ functional groups than −COOH and directly linked with the GCE surface by forming stable covalent bonds (C−N). The surface morphology demonstrated the successful adhering of the P-arg film to the GCE surface. The GO nanosheets were simultaneously reduced through an electrochemical deposition procedure. The electrodeposition of AuNSs along with GO as GO-AuNS nanocomposites was also performed by codeposition by the CV method without using reducing agent. A certain amount of GO (0.3 mg/mL) and AuNSs (3.0 mg/mL) were used for a dispersion for electrochemical deposition of rGO-AuNS nanocomposite. The CV was performed at a definite applied voltage range from −1.2 to +0.7 V and 50 mV s^{-1} was the scan rate for 14 CV cycles (Figure S6B). A N_2 gas bubbling was run for 10 min in the dispersion before running the CV electrodeposition.

The formation of the Go-AuNS nanocomposite layer on the GCE+P-arg surface was determined by observing the increased redox currents on the CV cycles. This rGO wrapped AuNS nanocomposite formed by simultaneous electrochemical reduction was comparatively high stable on the GCE/P-arg electrode surface because of its insoluble behavior in common solvents.[13] The AuNS nanoparticles were uniformly distributed and wrapped steadily by the rGO film. The homogeneous distribution of AuNSs throughout the rGO film is not only affected by the amount of AuNSs and GO nanosheets, but it also depends on the figure of CV cycles and the rate of scan. The high-resolution TEM images (Figure S6B) were very much consistent and indicated a distinct trapped of AuNSs inside the film of rGO nanosheets.

Electrochemical Characterization of GCE/P-arg/rGO-AuNS Nanocomposite Electrode. The bare and modified electrodes were electrochemically characterized by performing EIS methods (Figure 2) using 2 mM redox $[Fe(CN)_6]^{3-/4-}$ chemical diluted in 0.1 M KCl. The bare GC electrode showed the lowest EIS responses (Figure 2A) corresponding with redox solution $[Fe(CN)_6]^{3-/4-}$, whereas GCE+L-arg (Figure 2B), GCE+L-arg-AuNS (Figure 2C), and GCE+L-arg+ ErGO-

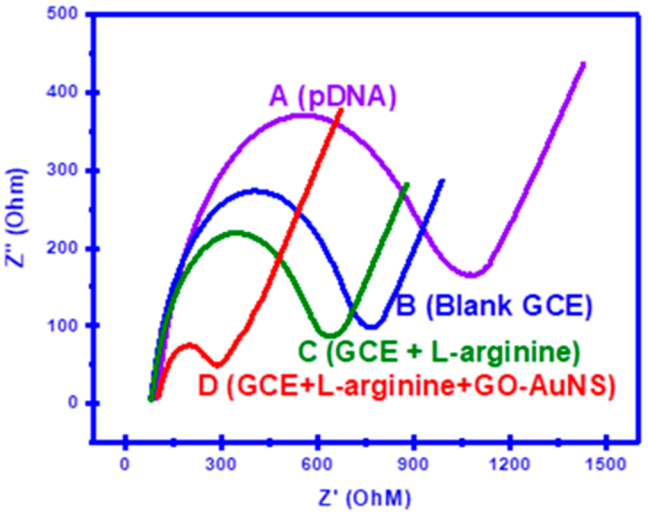

Figure 2. Nyquist plots of (A) blank GCE, (B) GCE+L-arginine, (C) GCE+rGO-AuNS, and (D) GCE+L-arginine+rGO-AuNS composite electrodes.

https://doi.org/10.1021/acsabm.2c00393
ACS Appl. Bio Mater. XXXX, XXX, XXX−XXX

AuNS (Figure 3D) modified electrodes demonstrated a higher catalytic response. The respective chemical reaction of

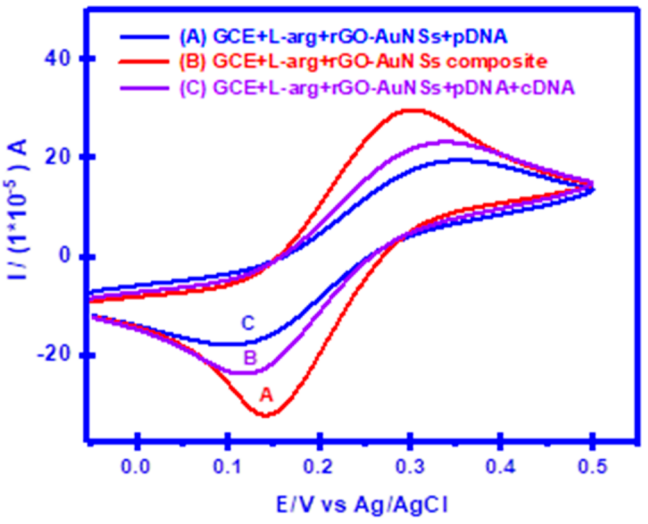

Figure 3. (A) CVs of the GCE+P-arg+ErGO-AuNS composite, (B) GCE+P-arg+ErGO-AuNS+pDNA, and (C) GCE+P-arg+ErGO-AuNS+dsDNA electrodes measured in 2 mM $[Fe(CN)6]^{3-/4-}$ solution containing 0.1 M KCl.

$[Fe(CN)_6]^{3-/4-}$ was enhanced notably by showing positive (+) charges of P-arg.[13] The significant signal current and the differences in potential suggested that the rGO-AuNS-modified electrode along with L-arg film catalyzed the surface effectively.[25] The individual connection of AuNSs with conductive graphene nanosheet can effectively enhance the conductivity for transferring the electrons quickly between the modified layer and the GCE surface.

The bare GC electrode showed the value of peak-to-peak separation (ΔE_p) 270 mV. The peak separation value of GCE +P-arg (ΔE_p = 185 mV) and GCE+P-arg+rGo-AuNS (ΔE_p = 82 mV) electrodes were decreased significantly. Therefore, the variation of peak separation value indicates an excellent catalytic property of GCE/P-arg/ErGO-AuNS sensor. The effective surface area of the bare GC and modified electrode surface was calculated by using Randles−Sevcik equation.

The electrochemical active surface area (A) was calculated for bare and modified electrodes based on the Randles−Sevcik equation.[26]

$$I_p = 2.69 \times 10^5 \cdot A D^{1/2} \eta^{3/2} \gamma^{1/2} C \quad (1)$$

In eq 1, A is denoted as the active surface area, the diffusion coefficient (D) is equal to 6.70 ± 0.02 × 10^{-6} cm^2/s, η is denoted as the number of electrons, the scan rate (V/s) of the CV system is denoted by γ, and C is defined as the probe DNA concentration (mol/cm^3). The values of active surface area (A) and modified GCE/p-Arg and GCE/P-arg/rGO-AuNS electrodes were figured out as 0.095, 0.165, and 0.335 cm^2, respectively. The results can explain the significant catalytic performance and higher surface area obtained by the modified GCE/P-arg/rGO-AuNS electrode.

Figure 2 shows the EIS spectrum, which were tested to confirm the electrochemical performance of the different modified electrodes. The EIS spectrum showed that the largest semicircle corresponds to the bare GC electrode, and appeared with an R_{ct} of 745 Ω in Figure 2A, reflecting the higher charge transfer resistance and lower electron transfer rate. GC/P-arg electrode showed 398 Ω R_{ct} value (Figure 2B). The electrode surface was modified by ErGO-AuNP composite and, as shown in Figure 2C, a smaller semicircle was observed when comparing with the bare and P-arg-only modified electrodes (R_{ct} value of 312 Ω) indicating a higher electrical conductivity of the surface. Furthermore, the electrode was modified by L-arginine+Go-AuNS (curve D) nanocomposite, obtaining an R_{ct} value of around 112 Ω and the lowest semicircle indicating the highest catalytic performance.

Electrocatalytic Influence of Poly(L-arginine) and rGO-AuNS Composite on the Electrochemical Measurements. The electrocatalytic performance of the fabricated biosensor for the detection of ctDNA is shown in figure. The electrochemical polymerization of L-arginine by the CV method is described in Figure S6A. The quasi-reversible redox of the CV voltammograms demonstrates the formation of a poly(L-arg) film on the GCE surface, which gradually increased in thickness with the number of the CV cycles. Figure 2A, B showed that the Nyquist plot of bare GCE was wider than that of the EIS semicircle of GCE+poly(L-arg), confirming the catalytic film formation on the GC electrode surface. The Nyquist plot of the GCE+Go-AuNS composite (Figure 2C) was smaller than both the bare and L-arg electrodes, which demonstrates that the L-arg and Go-AuNS composite had a positive influence on the electrochemical catalytic activity as shown in Figure 2.

Furthermore, the investigation of the catalytic influence of poly(L-arginine)+Go-AuNS nanocomposites was carried out by monitoring the R_{ct} value of EIS with 2 mM redox $[Fe(CN)6]^{3-/4-}$ in 0.1 M KCl solution (Figure 2). The catalytic behavior of different electrodes was also compared in the same procedure. The EIS signals of GCE+poly(L-arginine)+Go-AuNS composite electrodes were smaller than those EIS responses of bare GCE, L-arg, and Go-AuNS composite, which suggests a positive effectiveness of the electrochemical charge transfer rate. This may be the cause of the presence of physisorption attraction between the basal plane of the GO-AuNS composite and the L-arginine monomers with rich aromatic ring groups.[25,27] As a result, the higher number of nucleation sites were created and greatly enhanced the electropolymerization efficiency. The EIS response of the GCE+L-arginine+Go-AuNS composite electrodes (Figure 2D) showed a smaller R_{ct} value compared with that of both the poly(L-arginine) and Go-AuNS nanocomposite (Figure 2B, C), proving that addition of L-arginine significantly improved the electrochemical charge transfer efficiency of the Go-AuNS nanocomposite.

Switching Behavior Observing the Immobilization and Hybridization of DNA. The performance of our newly designed biosensors was studied by electrochemical methods in 2 mM redox $[Fe(CN)6]^{3-/4-}$ containing 0.1 M KCl solution (Figure 3). The fabricated sensor (GCE+P-arg+ErGO-AuNS) showed an excellent electrocatalytic performance in a neutral measurements (Figure 3A). Probe ssDNA was immobilized on the fabricated GCE surface after the treatment with EDC/NHS coupling method. A noncovalent bonding was formed on the surface between the ErGO-AuNS composite and the nucleobases ring.[28] After the immobilization of probe DNA, the redox current of the biosensor (GCE+P-arg+ErGO-AuNS +pDNA) decreased significantly (Figure 3C). The immobilized probe DNA acts as random coils and has flexible

https://doi.org/10.1021/acsabm.2c00393
ACS Appl. Bio Mater. XXXX, XXX, XXX−XXX

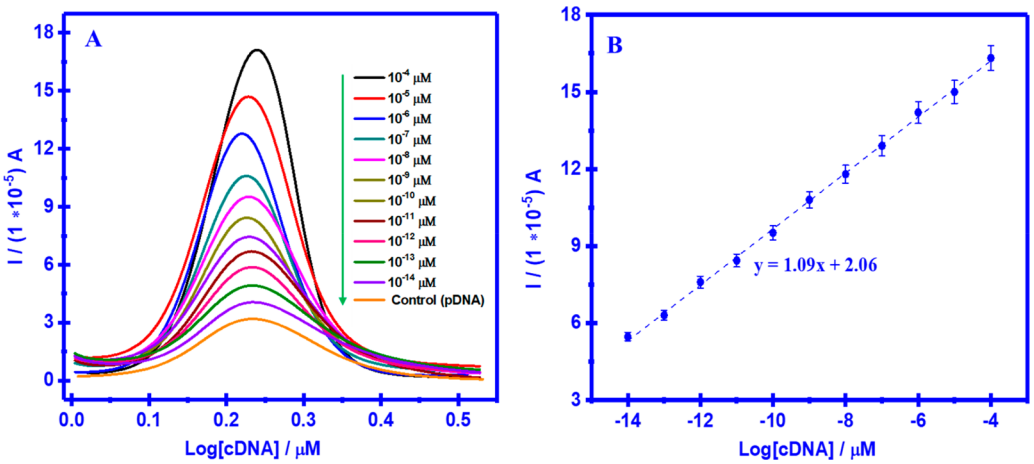

Figure 4. (A) DPV voltammogram and (B) obtained calibration curves for different concentrations of ctDNA using GCE+P-arg+ErGO-AuNS sensor in PBS buffer solution (pH 7.4) at a 50 mV/s scan rate with a wide range of concentrations from 1×10^{-4} to 1×10^{-14} μM (A).

Table 1. Comparison of the Electrochemical Biosensor Performance for the ctDNA Detection with Reported Works from the Year 2014 to 2019

methods	surface modification technique	target detection	linear response range	LOD	stability (days)	ref
electrochemical	poly(L-arg)/rGO-AuNSs on the GC electrode	ctDNA	1×10^{-20} to 1×10^{-10} M	1×10^{-20} M	30	this work
electrochemical	rGO/AuNS nanocomposite on the GC electrode	ctDNA	$1 \times 10^{-20}$to 1×10^{-12} M	1×10^{-20} M	20	21
electrochemical	poly-xanthurenic acid/MoS_2 composite on CP electrode	ctDNA	1×10^{-16} - 1×10^{-10} M	1×10^{-17} M	7	9
electrochemical	thin layer MoS_2/graphene composite on GC electrode	ctDNA	1×10^{-16} to 1×10^{-13} M	1×10^{-17} M		3
electrochemical	DNA clutch probes (DCPs)/ nanostructured microelectrodes equipped with PNA probe clamps	ctDNA		1 fg/μL		7
electrochemical	AuNP/PNA probes	ctDNA	50−3200 fM	50 fM		5

characteristics, which may confirm the immobilization event and hinder the electron transfer pathway.[29]

Therefore, the response of the biosensor (GCE+P-arg +ErGO-AuNS+pDNA) was declined, hereby defined as "signal-off" phenomena. The immobilized single probe was then attached with ctDNA through a hybridization protocol. A significant increase redox signal (Figure 3B) was obtained after hybridization compared with the immobilization signal. The double stranded DNA conjugate was formed by the hybridization event and released from the electrode surface. This enhanced the regeneration of the redox signal, which is considered as the "signal-on" mode.[30] A stable hydrogen bond was formed after the hybridization between the nucleobases and the phosphate sugar backbone that enhanced the dsDNA release from the electrode surface.[31] The switching phenomena of this biosensor by immobilization and hybridization was revealed as a potential and reliable ctDNA biomarker identification tool, without using any labels or any other indicator of the hybridization events.

Quantitative Analysis of Target DNA Sequences. The catalytic signal changes of various concentrations of ctDNA hybridization were determined by the DPV method in a wide range of potential. The GCE+P-arg+ErGO-AuNS+ssDNA electrode was used for the detection of the ctDNA sequences. The resulting DPV voltammogram is depicted in Figure 4A. The increasing trend of DPV oxidation current with the ctDNA concentration was considered as the measurement signal. The oxidation current was linearly fitted with the logarithmic value of the ctDNA concentrations. The ctDNA concentration range was used in this study from 1.0×10^{-20} M to 1.0×10^{-10} M (R^2 = 0.998) (Figure 4B). The LOD was determined to be 1.0×10^{-20} M (S/N = 3).

The biosensor achieved a wider dynamic range for ctDNA detection in comparison with previously reported methods (Table 1). This is because the nanosized range spherical L-arg +ErGO-AuNS composite particles were highly dispersed in a single layer and acted as a DNA immobilization carrier matrix. The rGO-AuNS composite containing the rich carboxylic acid layer provided a large active binding area, facilitating the DNA probe immobilization on the GCE. This also made a maximally covered surface area of the DNA acceptive layer. Therefore, the sandwich type assay of AuNSs with the polymeric bedded rGO nanosheets on the GCE significantly amplified the catalytic performance of the hybridization of DNA, and this rendered highly sensitive detection of the DNA biosensor.

Our sensor was compared with other reported works (Table 1) with different biosensor methods reported in the past few years for the *PIK3CA* gene biomarker detection of the ctDNA. Our fabricated polymeric bedded noble metal biosensor showed a significant ultrasensitivity with a low detection limit.

Selectivity Study of DNA Hybridization Recognition. The fabricated noble metal-based biosensor was significantly selective and specific for the sensitive detection of the ctDNA liquid biopsy biomarker. The selectivity study accomplished to hybridize the ssDNA capture probe with the complementary target, noncomplementary and mismatched sequences. EIS signal variation of various oligos modified GCE in redox $[Fe(CN)_6]^{3-/4-}$ solution is listed in Figure 5. The R_{et} value

https://doi.org/10.1021/acsabm.2c00393
ACS Appl. Bio Mater. XXXX, XXX, XXX−XXX

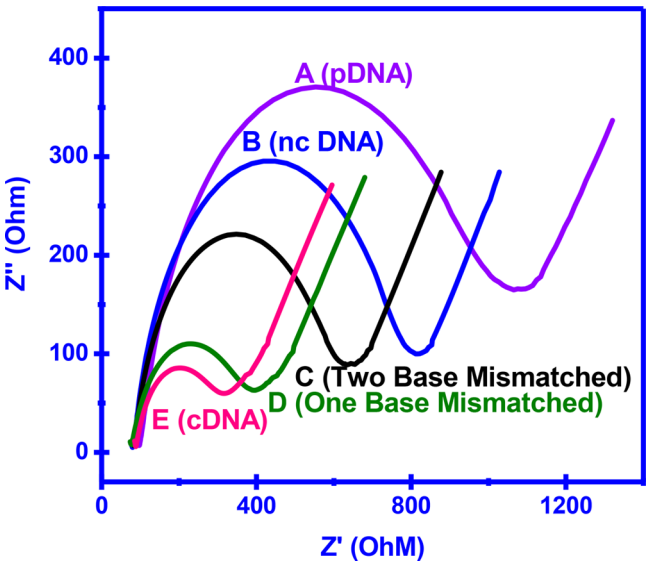

Figure 5. Nyquist plot of various modified electrodes measured in 0.1 M KCl containing 2 mM $[Fe(CN)_6]^{3-/4-}$ solution for (A) GCE+P-arg +ErGO-AuNS+ssDNA, (E) GCE+P-arg+ErGO-AuNS + dsDNA, (B) hybridized with ncDNA, (C) two-base mismatched DNA, and (D) one-base mismatched DNA.

increased significantly after loading the ssDNA probe onto the GCE/P-arg/ErGO-AuNS electrode surface, confirming the complete immobilization of the probe DNA on the matrixes (Figure 5A). The R_{et} value decreased massively (Figure 5E) after loading the complementary target DNA on the GCE/P-arg/ErGO-AuNS/ssDNA surface, as the probe DNA hybridized with the target and released the hybridized dsDNA conjugates from the surface, obtaining the "signal-on" phenomena.[32]

The hybridization of the ssDNA probe with the ncDNA caused minor changes in the R_{et} value (Figure 5B) compared with the probe DNA immobilization electrode, indicating the lack of hybridization events and far from the ctDNA hybridization response. The R_{et} values of one-base (Figure 5D) and two-base (Figure 5C) mismatched DNA were slightly different and higher than those of complementary DNA hybridization. The results supported the incomplete hybridization of one-base and two-base mismatched DNA. This study demonstrated that the fabricated label-free electrochemical sensor showed an excellent selectivity and specificity toward the ctDNA biomarker of gastric cancer detection.

Study of Stability and Reproducibility. The stability of the developed sensor was determined by considering the DPV responses of fabricated GCE+P-arg+ErGO-AuNS electrode. The fabricated electrodes were kept at 4 °C in the refrigerator for a period of 4 weeks and were analyzed during that time.

The DPV signal decreased around 2.2% after 5 days of storage, indicating that the DNA sensor had favorable stability. Nearly 94 and 82% current response was retained of the initial DPV value of the sensors after being kept 2 and 3 weeks stored under the same conditions, which demonstrated an excellent stability (see S5 in the Supporting Information). 1.0×10^{-20} M target sequences was detected for the measurement of reproducibility of this biosensor with five equivalently made probe-modified GCE. The results showed that a change in the response of RSD of 4.5 ± 0.1% (n = 5) was determined. This indicates that our fabricated DNA sensor is associated with an excellent reproducibility for ctDNA biomarker detection. This study demonstrates that the proposed electrochemical DNA based method can be effective for highly authentic, precise, and specific detection of ctDNA in clinical and environmental analysis.

Clinical Sample Examination. As shown in Table 2, we detected 14 samples with the *PIK3CA* gene and 2 with the *PIK3CA* gene mutation in 60 clinical ctDNA samples from gastric cancer patients by using the developed biosensor; those results were the same as the clinical sample sequencing results. Sorafenib was recommended for use in target therapy for the 14 patients who were positive for the *PIK3CA* gene, and 5-Aza was recommended for use in therapy for the two patients with the *PIK3CA* gene mutation.

Table 2. Examination Results of the *PIK3CA* Gene in 60 Gastric Cancer Patients

patient no.	age	sex	clinical diagnosis	*PIK3CA* gene mutation	*PIK3CA* gene positive
15	60−70	man	advanced gastric cancer	2	1
13	55−60	female	Middle gastric cancer	0	2
12	50−55	man	Middle gastric cancer	0	4
10	45−50	female	Middle gastric cancer	0	2
5	40−45	man	early gastric cancer	0	3
5	40−45	female	early gastric cancer	0	2

CONCLUSION

In this study, a high-performance DNA-based electrochemical sensor was fabricated for the detection of the *PIK3CA* gene of ctDNA. For this purpose, we used well-defined surface modification chemistry consisting of the electrodeposition of an rGO-AuNS nanocomposite supported by a poly(L-arginine) polymeric film on the GCE electrode surface. The resulting L-arg+ErGO-AuNS nanocomposite sensing platform achieved a good biocompatibility and showed an excellent electrochemical transduction activity in favorable conditions. The sensing platform immobilized the DNA probe through $\pi-\pi$ interaction between the rings of DNA bases, making a "switching-off" mode sensor by increasing the charge transfer resistance. After the hybridization event, the resulting dsDNA conjugate was released from the L-arg+rGO-AuNS nanocomposite platform. This facilitated a decrease of the charge transfer resistance, or a "switching-on" mode. The developed electrochemical DNA sensor was successfully implemented for amplifying the gastric cancer biomarker *PIK3CA* gene of ctDNA. The biosensor showed an excellent selectivity, sensitivity, reproducibility and stability toward the detection of the target biomarker. Our DNA sensor also demonstrated a wider linear response range of ctDNA concentrations, from 1.0×10^{-20} M to 1.0×10^{-10} M (R^2 = 0.997), with a limit of detection of 1.0×10^{-20} M. This straightforward and simple fabrication and label-free detection protocol possess a great potential for applications in clinical diagnostics and biomedical analysis. Hence, the designed GCE/L-arg/ErGO-AuNS nanocomposite platforms are an effective and promising with a low-cost detecting

https://doi.org/10.1021/acsabm.2c00393
ACS Appl. Bio Mater. XXXX, XXX, XXX−XXX

method for the analysis of liquid biopsy of gastric cancer biomarkers for biomedical applications. Long-term biocompatibility of the fabricated biosensor and the detection protocol of L-arg/ErGO/AuNS nanohybrids associated with other biomarker detection applications are further suggested by the broad studies. The developed ctDNA sensor can be further developed for a sustainable, fifth-generation, advanced point-of-care device prototype that provides great efficient detection with the aspects of biocompatibility, cost-effectiveness, portability, and wearability for use in smart sensor technology, intelligent health care, pandemic prevention, and other global public health uses.[33]

■ ASSOCIATED CONTENT

Supporting Information

The Supporting Information is available free of charge at https://pubs.acs.org/doi/10.1021/acsabm.2c00393.

Data for optimization of the L-arginine concentration for electropolymerization, optimization of the electropolymerization cycle of L-arginine, optimization of the potential window for the electropolymerization of L-arginine, optimization of the L-arg deposition protocol, and data for the stability and reproducibility study (PDF)

■ AUTHOR INFORMATION

Corresponding Author

Daxiang Cui − *Institute of Nano Biomedicine and Engineering, School of Sensing Science and Engineering, Shanghai Jiao Tong University, Shanghai 200240, PR China; National Engineering Center for Nanotechnology, Shanghai 200241, PR China;* orcid.org/0000-0003-4513-905X; Phone: 0086-21-34206886; Email: dxcui@sjtu.edu.cn

Authors

Mahbubur Rahman − *Institute of Nano Biomedicine and Engineering, School of Sensing Science and Engineering, Shanghai Jiao Tong University, Shanghai 200240, PR China; Department of General Educational Development, Faculty of Science and Information Technology (FSIT), Daffodil International University, Dhaka 1341, Bangladesh;* orcid.org/0000-0002-7921-9288

Jiaqi Niu − *Institute of Nano Biomedicine and Engineering, School of Sensing Science and Engineering, Shanghai Jiao Tong University, Shanghai 200240, PR China*

Xinyuan Cui − *Medical Imaging Department of Tong Ji Hospital Affiliated to Tongji University, Shanghai 200065, PR China*

Cheng Zhou − *Institute of Nano Biomedicine and Engineering, School of Sensing Science and Engineering, Shanghai Jiao Tong University, Shanghai 200240, PR China; National Engineering Center for Nanotechnology, Shanghai 200241, PR China*

Ning Tang − *Institute of Nano Biomedicine and Engineering, School of Sensing Science and Engineering, Shanghai Jiao Tong University, Shanghai 200240, PR China*

Han Jin − *Institute of Nano Biomedicine and Engineering, School of Sensing Science and Engineering, Shanghai Jiao Tong University, Shanghai 200240, PR China; National Engineering Center for Nanotechnology, Shanghai 200241, PR China;* orcid.org/0000-0001-7427-4600

Complete contact information is available at: https://pubs.acs.org/10.1021/acsabm.2c00393

Funding

This work was supported by Key Basic Research Program of China (2017YFA0205304), Nature Scientific Foundation of China (82020108017, 81921002, and 81602184), and Medical Engineering Cross Project of Shanghai Jiao Tong University (YG2016ZD10, ZH2018QNA51, ZH2018QNA28). This work was also supported by "the Belt and Road" young scientist exchange program, Shanghai (Grant 18410741600), Shanghai Natural Science Foundation (Grant 86973) and Oceanic Interdisciplinary Program of Shanghai Jiao Tong University (Grant BX2020208).

Notes

The authors declare no competing financial interest.

■ ACKNOWLEDGMENTS

This work was generously supported by KBR Program of China, NSF of China, and MEC Project of Shanghai Jiao Tong University. The authors acknowledge "the Belt and Road" young scientist exchange program of the Science and Technology Commission of Shanghai, and Oceanic Interdisciplinary Program of Shanghai Jiao Tong University. The authors also thank Dr. Gabriel Alfranca for his comments and corrections.

■ REFERENCES

(1) Torre, L. A.; Bray, F.; Siegel, R. L.; Ferlay, J.; Lortet-Tieulent, J.; Jemal, A. Global cancer statistics, 2012. *CA: a cancer journal for clinicians* **2015**, *65* (2), 87−108.

(2) Cristescu, R.; Lee, J.; Nebozhyn, M.; Kim, K.-M.; Ting, J. C.; Wong, S. S.; Liu, J.; Yue, Y. G.; Wang, J.; Yu, K.; et al. Molecular analysis of gastric cancer identifies subtypes associated with distinct clinical outcomes. *Nature medicine* **2015**, *21* (5), 449.

(3) Chu, Y.; Cai, B.; Ma, Y.; Zhao, M.; Ye, Z.; Huang, J. Highly sensitive electrochemical detection of circulating tumor DNA based on thin-layer MoS_2/graphene composites. *RSC Adv.* **2016**, *6* (27), 22673−22678.

(4) Indrasekara, A. S. D. S.; Meyers, S.; Shubeita, S.; Feldman, L. C.; Gustafsson, T.; Fabris, L. Gold nanostar substrates for sers-based chemical sensing in the femtomolar regime. *Nanoscale* **2014**, *6* (15), 8891−8899.

(5) Nguyen, A. H.; Sim, S. J. Nanoplasmonic biosensor: Detection and amplification of dual bio-signatures of circulating tumor DNA. *Biosens. Bioelectron.* **2015**, *67*, 443−449.

(6) Yong, E. Written in Blood. *Nature* **2014**, *511* (7511), 524.

(7) Das, J.; Ivanov, I.; Sargent, E. H.; Kelley, S. O. DNA clutch probes for circulating tumor DNA analysis. *J. Am. Chem. Soc.* **2016**, *138* (34), 11009−11016.

(8) Rusling, J. F.; Kumar, C. V.; Gutkind, J. S.; Patel, V. Measurement of biomarker proteins for point-of-care early detection and monitoring of cancer. *Analyst* **2010**, *135* (10), 2496−2511.

(9) Zhang, W.; Dai, Z.; Liu, X.; Yang, J. High-performance electrochemical sensing of circulating tumor DNA in peripheral blood based on poly-xanthurenic acid functionalized MoS_2 nanosheets. *Biosens. Bioelectron.* **2018**, *105*, 116−120.

(10) Cui, H.-F.; Cheng, L.; Zhang, J.; Liu, R.; Zhang, C.; Fan, H. An electrochemical DNA sensor for sequence-specific DNA recognization in a homogeneous solution. *Biosens. Bioelectron.* **2014**, *56*, 124−128.

(11) Rahman, M.; Heng, L. Y.; Futra, D.; Ling, T. L. Ultrasensitive Biosensor for the Detection of Vibrio cholerae DNA with Polystyrene-co-acrylic Acid Composite Nanospheres. *Nanoscale Res. Lett.* **2017**, *12* (1), 474.

(12) Rahman, M.; Heng, L. Y.; Futra, D.; Chiang, C. P.; Rashid, Z. A.; Ling, T. L. A highly sensitive electrochemical DNA biosensor from

acrylic-gold nano-composite for the determination of arowana fish gender. *Nanoscale Res. Lett.* **2017**, *12* (1), 484.
(13) Khan, M.; Liu, X.; Tang, Y.; Liu, X. Ultra-sensitive electrochemical detection of oxidative stress biomarker 8-hydroxy-2′-deoxyguanosine with poly (L-arginine)/graphene wrapped Au nanoparticles modified electrode. *Biosens. Bioelectron.* **2018**, *117*, 508−514.
(14) Tığ, G. A. Development of electrochemical sensor for detection of ascorbic acid, dopamine, uric acid and l-tryptophan based on Ag nanoparticles and poly (l-arginine)-graphene oxide composite. *J. Electroanal. Chem.* **2017**, *807*, 19−28.
(15) Yi, Y.; Zhu, G.; Wu, X.; Wang, K. Highly sensitive and simultaneous electrochemical determination of 2-aminophenol and 4-aminophenol based on poly (l-arginine)-β-cyclodextrin/carbon nanotubes@ graphene nanoribbons modified electrode. *Biosens. Bioelectron.* **2016**, *77*, 353−358.
(16) Hasanzadeh, M.; Mokhtari, F.; Shadjou, N.; Eftekhari, A.; Mokhtarzadeh, A.; Jouyban-Gharamaleki, V.; Mahboob, S. Poly arginine-graphene quantum dots as a biocompatible and non-toxic nanocomposite: layer-by-layer electrochemical preparation, characterization and non-invasive malondialdehyde sensory application in exhaled breath condensate. *Materials Science and Engineering: C* **2017**, *75*, 247−258.
(17) Bollella, P.; Fusco, G.; Tortolini, C.; Sanzò, G.; Favero, G.; Gorton, L.; Antiochia, R. Beyond graphene: electrochemical sensors and biosensors for biomarkers detection. *Biosens. Bioelectron.* **2017**, *89*, 152−166.
(18) Bhardwaj, S. K.; Mujawar, M.; Mishra, Y. K.; Hickman, N.; Chavali, M.; Kaushik, A. Bio-inspired graphene-based nano-systems for biomedical applications. *Nanotechnology* **2021**, *32* (50), 502001.
(19) Zhang, A.; Liu, Q.; Huang, Z.; Zhang, Q.; Wang, R.; Cui, D. Electrochemical Cytosensor Based on a Gold Nanostar-Decorated Graphene Oxide Platform for Gastric Cancer Cell Detection. *Sensors* **2022**, *22* (7), 2783.
(20) Rahman, M.; Cui, D.; Zhou, S.; Zhang, A.; Chen, D. A graphene oxide coated gold nanostar based sensing platform for ultrasensitive electrochemical detection of circulating tumor DNA. *Analytical Methods* **2020**, *12*, 440−447.
(21) Zhang, A.; Chang, J.; Chen, Y.; Huang, Z.; Alfranca, G.; Zhang, Q.; Cui, D. Spontaneous implantation of gold nanoparticles on graphene oxide for salivary SERS sensing. *Analytical Methods* **2019**, *11*, 5089−5097.
(22) Chen, Y.; Zhang, Y.; Pan, F.; Liu, J.; Wang, K.; et al. Breath Analysis Based on Surface-Enhanced Raman Scattering Sensors Distinguishes Early and Advanced Gastric Cancer Patients from Healthy Persons. *ACS Nano* **2016**, *10*, 8169−8179.
(23) Liang, S.; Li, C.; Zhang, C.; Chen, Y.; Xu, L.; Bao, C.; Wang, X.; liu, G.; zhang, F.; Cui, D. CD44v6Monoclonal Antibody-Conjugated Gold Nanostars for Targeted Photoacoustic Imaging and Plasmonic Photothermal Therapy of Gastric Cancer Stem-like Cells. *THERANOSTICS* **2015**, *5*, 970−984.
(24) Mohiuddin, M.; Arbain, D.; Islam, A.K.M.; Rahman, M.; Ahmad, M.S.; Ahmad, M.N. Covalent immobilization of α-glucosidase enzyme onto amine functionalized multi-walled carbon nanotubes. *Current Nanoscience* **2014**, *10* (5), 730−735.
(25) Zhang, W.; Liu, J.; Niu, W.; Yan, H.; Lu, X.; Liu, B. Tip-selective growth of silver on gold nanostars for surface-enhanced Raman scattering. *ACS Appl. Mater. Interfaces* **2018**, *10* (17), 14850−14856.
(26) De Silva Indrasekara, A. S.; Johnson, S. F.; Odion, R. A.; Vo-Dinh, T. Manipulation of the Geometry and Modulation of the Optical Response of Surfactant-Free Gold Nanostars: A Systematic Bottom-Up Synthesis. *ACS omega* **2018**, *3* (2), 2202−2210.
(27) Zhou, X.; Jing, W.; Zhuang, Z.; Zheng, X. In Situ synthesis of gold nanoparticles on poly (L-arginine) modified glassy carbon electrode and electrocatalytic oxidation of glucose in alkaline solution. *ECS Electrochemistry Letters* **2015**, *4* (8), G5−G7.
(28) Du, J.; Yue, R.; Ren, F.; Yao, Z.; Jiang, F.; Yang, P.; Du, Y. Novel graphene flowers modified carbon fibers for simultaneous determination of ascorbic acid, dopamine and uric acid. *Biosens. Bioelectron.* **2014**, *53*, 220−224.
(29) Wang, X.; Ma, W.; Ge, T.; Yang, T.; Jiao, K. A reductively treated thin layer MoS2 nanosheet-poly (xanthurenic acid) composite with dramatically enhanced electrochemical performance and extended sensing applications. *Electrochim. Acta* **2016**, *190*, 1025−1031.
(30) Liu, S.; Wang, L.; Luo, Y.; Tian, J.; Li, H.; Sun, X. Polyaniline nanofibres for fluorescent nucleic acid detection. *Nanoscale* **2011**, *3* (3), 967−969.
(31) Hu, Y. W.; Yang, T.; Wang, X. X.; Jiao, K. Highly Sensitive Indicator-Free Impedance Sensing of DNA Hybridization Based on Poly (m-aminobenzenesulfonic acid)/TiO_2 Nanosheet Membranes with Pulse Potentiostatic Method Preparation. *Chemistry−A European Journal* **2010**, *16* (6), 1992−1999.
(32) Yang, T.; Guan, Q.; Guo, X.; Meng, L.; Du, M.; Jiao, K. Direct and freely switchable detection of target genes engineered by reduced graphene oxide-poly (m-aminobenzenesulfonic acid) nanocomposite via synchronous pulse electrosynthesis. *Analytical chemistry* **2013**, *85* (3), 1358−1366.
(33) Chaudhary, V.; Kaushik, A. K.; Furukawa, H.; Khosla, A. Towards 5th generation AI and IoT driven sustainable intelligent sensors based on 2d Mxenes and borophene. *ECS Sensors* **2022**, *1*, No. 013601.

https://doi.org/10.1021/acsabm.2c00393
ACS Appl. Bio Mater. XXXX, XXX, XXX−XXX